Second-harmonic green generation from two-dimensional $\chi^{(2)}$ nonlinear photonic crystal with orthorhombic lattice structure

L.-H. Peng,[a] C.-C. Hsu, and Y.-C. Shih
Department of Electrical Engineering and Institute of Electro-Optical Engineering, National Taiwan University, Taipei, Taiwan, Republic of China

(Received 20 March 2003; accepted 2 September 2003)

We report the synthesis of nonlinear photonic crystals (NPCs) with a periodical distribution of inverted $\chi^{(2)}$ nonlinearity having an orthorhombic lattice structure on Z-cut congruent-grown lithium niobate ($LiNbO_3$) substrate. The quasiphase-matching (QPM) mechanism of nonlinear wave interaction is examined by monitoring the far-field emission pattern of second-harmonic generation (SHG) as the NPC is pumped by a Nd:yttrium–aluminum–garnet laser beam. We observe (i) a series distribution of green SHG in a direction transverse to the fundamental beam, and (ii) an increase of phase-matching temperature in the SHG peak signal with the azimuth rotation angle in the $x-y$ plane. These observations are ascribed to the high-order reciprocal lattice vectors assisted QPM–SHG process in a NPC that has a distribution of $\chi^{(2)}$ nonlinearity with an orthorhombic crystal symmetry. © *2003 American Institute of Physics.*
[DOI: 10.1063/1.1622786]

Photonic crystals (PCs) are known for their capability to manipulate the light localization and emission properties such that optical function of switch[1] and laser,[2] and enhanced nonlinearity for solitary wave[3] and frequency conversion[4] can be resultant. These phenomena can be ascribed to a unique dispersion of photonic subbands in the crystal.[5] Current technology has shown that linear or nonlinear PCs can be constructed by maximizing the index contrast in a periodical modulation of either or both $\chi^{(1)}$ and $\chi^{(2)}$ in the constituent materials[6] or via Kerr nonlinearity[7] at a lattice spacing on the order of optical wavelength (λ/n). To reduce the stringent requirement of size control in the unite cell construction, another class of nonlinear photonic crystals (NPCs) has been proposed. In such NPC one maintains a constant dielectric function in space but periodically reverses the sign of $\boldsymbol{\chi}^{(2)}$ nonlinear tensor at every coherent length $l_c = \lambda_\omega/4(n_{2\omega}-n_\omega)$.[8] The reciprocal lattice vector $\mathbf{G}$ of a NPC can further support a momentum conservation mechanism, i.e., via quasiphase-matching (QPM) of $\mathbf{k}_1+\mathbf{k}_2=\mathbf{k}_3+\mathbf{G}$ to ensure energy conversion among the interacting waves of vectors $\mathbf{k}_1$, $\mathbf{k}_2$, and $\mathbf{k}_3$ when the corresponding Fourier component of $\boldsymbol{\chi}^{(2)}(\mathbf{G})$ has a nonzero value.[9,10]

Here we report the synthesis, characterization, and analysis of QPM–NPCs with orthorhombic lattice site on lithium niobate ($LiNbO_3$) substrate. We note a series of green second-harmonic generation (SHG) can be excited in a direction transverse to the fundamental Nd:yttrium–aluminum–garnet (YAG) laser pump beam. The phase-matching temperature (T) of the peak SHG signal is found to increase with the azimuth rotation angle (ϕ) of the crystal but decrease with the lattice spacing. These observations can be ascribed to a unique dispersion of $\mathbf{G}_{mn}(T,\phi)$ in the QPM–NPCs and suggestive of promising nonlinear optical applications for two-dimensional (2D) wave front engineering[11] and coherent light deflection.[12]

The including of a QPM scheme on NPC can further enable a direct access to the largest tensor component in $\boldsymbol{\chi}^{(2)}$.[13] This mechanism differs from that of conventional birefringent phase matching by allowing the interacting waves to polarize in the same direction and thus lead to a maximum use of the nonlinearity effect due to the enhanced overlap of optical field in space.[14] A physical mechanism that can cause a periodical sign reversal of $\boldsymbol{\chi}^{(2)}$ in crystal can also render a polarity change in $\mathbf{P}_s$ as well.[15] This effect suggests that one can take advantage of the reversible polarization status of $\mathbf{P}_s$ in the ferroelectric domains, i.e., via domain reversal, to realize a QPM–NPC.[16] To initiate such a polarization switching process, one can conveniently apply an electric field to overcome the crystal's coercive field (E_c) and to nucleate an inverted domain on the polar surface.[17] With additional supply of switching current of $2AdP_s/dt$ via an external circuit, one can further compensate the depolarization field in bulk crystal and result in the stabilization of inverted crystallite with area A.[18]

Albeit electrical poling has been regarded as a mature technique to produce bulk single domain ferroelectric crystals,[19] an extension of this method to make an arrangement of rod- or grid-like $\boldsymbol{\chi}^{(2)}$ crystallites and register them in a two- or three-dimensional lattice structure to form a QPM–NPC still remains a great challenge. One such difficulty arises from the existence of large internal field (E_{int}) due to the nonstoichiometric defects for crystals grown from the melt. The E_{int} value amounts to 15%–25% of E_c in the widely used lithium niobate ($LiNbO_3$)[20] and lithium tantalate ($LiTaO_3$)[21] nonlinear crystals of congruent composition. Such a giant internal field can cause a serious back switching of inverted domains as one terminates the poling field.[18] The most troublesome, however, is the loss of $\boldsymbol{\chi}^{(2)}$ patterning and therefore the destruction of nonlinear photonic structure due to the incontrollable merging of inverted domains. Such an unwelcome domain motion is caused by an inherent fringing field effect when the corrugated ferroelectric surface covered

[a]Electronic mail: peng@cc.ee.ntu.edu.tw

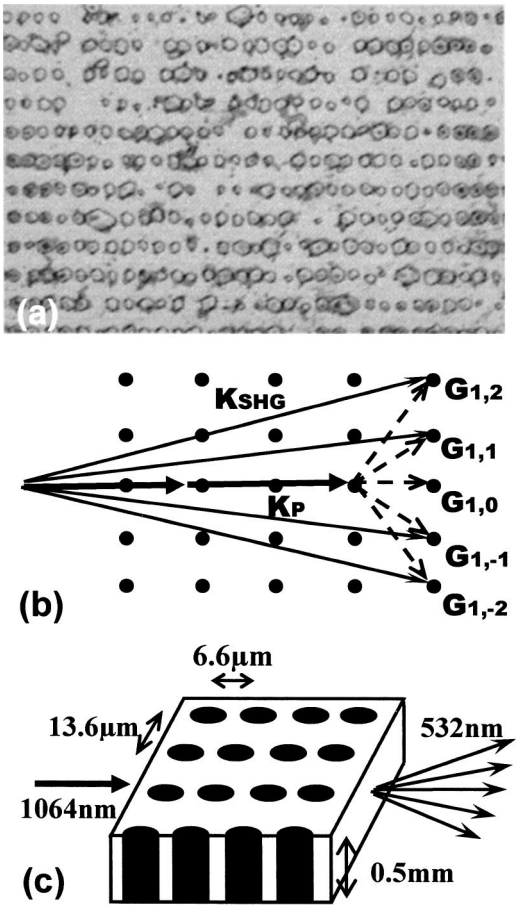

FIG. 1. (a) Etched-Z face micrograph showing a rod-like distribution of $\chi^{(2)}$ NPC on 500-μm-thick $LiNbO_3$ with a 2D periodicity of $6.6\times13.6\ \mu m^2$. (b) QPM–SHG process in the reciprocal space of NPC having an orthorhombic lattice structure. (c) Schematic draw of wave propagation and generation in the $\chi^{(2)}$ NPC of (a).

with a photo-resist pattern is subject to a field action (E_z).[22]

We have recently shown that an electrostatic compensation mechanism to counteract the aforementioned tangential field effect can be effectively realized by surrounding the $\chi^{(2)}$ lattice site with a sheet of positive charge prior to initiate the electrical poling.[23] Our device processing steps begin by letting an aluminum (Al)-patterned $LiNbO_3$ substrate undergone a heat treatment at 1050 °C for 5 h. The microfissure formed in the oxidized Al_2O_3 pattern during the heat treatment can further provide an electric contact path to the underlying $LiNbO_3$ and therefore can initiate the nucleation of inverted domain at the designated lattice site. The capability of (i) selectively nucleating the inverted domain, and (ii) restricting the transverse motion of inverted domain constitutes the major advantages in our construction of $\chi^{(2)}$ QPM–NPCs.

Illustrated in Fig. 1(a) is a $-Z$ face micrograph of a NPC showing a rod-like distribution of $\chi^{(2)}$ nonlinearity with a 2D periodicity of $6.6\times13.6\ \mu m^2$. A close examination of the etched micrograph indicates that such rods, with an inverted area as small as $3.3\times3.3\ \mu m^2$, indeed are resided on the rectangular (i.e., orthorhombic) lattice site and periodically distributed in the $x-y$ plane. The observation of periodically poled inverted domains with a high aspect ratio over 150 on a 500-μm-thick substrate has proven the use of the two-step poling process in the synthesis of $\chi^{(2)}$ NPCs.

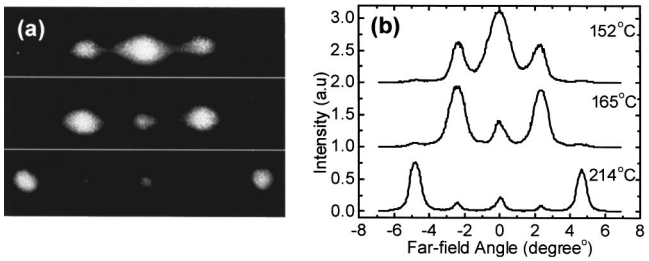

FIG. 2. (a) CCD image, and (b) far-field intensity pattern of a $6.6\times13.6\ \mu m^2$ QPM–SHG NPC pumped by a Nd:YAG at 152, 165, and 214 °C, respectively, and at normal incidence configuration.

We further note the spatial distribution of $\chi^{(2)}$ nonlinearity in the NPC of Fig. 1(a) has a structure symmetry (C_{2v}) different from that of C_{3v} in the host crystal of $LiNbO_3$. This would affect the generation and propagation of nonlinear interacting waves in the QPM process as shown in Figs. 1(b) and 1(c), respectively. In order to examine such effects, we use the SHG technique to monitor the intensity distribution in the far-field emission pattern as the incident angle of the pump laser and the crystal temperature of NPC are changed. A fundamental pump beam of Nd:YAG laser with ~10 ns pulse width (New Wave Technology, USA) was lightly focused onto the end-facet polished sample. An in-house temperature controller unit was attached to a rotation stage which allows a variation of crystal temperature from 5 to 240 °C and a change of incident angle to ±15°.

First shown in Fig. 2 are the (a) charge coupled device (CCD) images, and (b) corresponding far-field intensity distribution of the SHG signals taken from the $6.6\times13.2\ \mu m^2$ period sample and at a crystal temperature of 152, 165, and 214 °C, respectively. The data were measured at a normal incident configuration with the pump Nd:YAG laser beam (of a peak intensity~2 MW/cm^2) propagating along the short period (i.e., 6.6 μm) side of the NPC sample. Albeit the green SHG resembles that in the conventional one-dimensional (1D)–QPM PPLN,[22] the appearance of a series of SHG signals with *unequal* intensity signifies the participation of *transverse* reciprocal lattice vectors, as shown in Fig. 1(b), that are absent in the 1D case. Moreover, as one increases the crystal temperature, an interesting shift of the SHG peak intensity to a larger far-field angle, i.e., from 0° to 4.5°, can be clearly resolved. These phenomena suggest that the high-order transverse reciprocal lattice vector becomes dominant in the nonlinear interaction of QPM–SHG process as one increases the crystal temperature.

In order to grant a further understanding of the earlier mechanism, we slightly rotate the crystal in the $x-y$ plane such that various reciprocal lattice vectors and their nonlinear activities can be addressed. Illustrated in Fig. 3 are the (a) CCD images, and (b) far-field intensity of the SHG signals taken from another QPM–NPC sample having a larger period of $6.9\times13.6\ \mu m^2$. The data were measured at a crystal temperature of 10 °C and an azimuth rotation angle of $\phi=0°$ and ±1.45°, respectively. Note the SHG patterns in the $\phi=\pm1.45°$ measurements take a mirror image to each other. This leads to an observation of peak SHG signal at a far-field angle of ±2.3° but overlaid with discrete weak green spots that appear not phase matched. In the normal incident condition ($\phi=0°$), however, only weak SHG signals can be

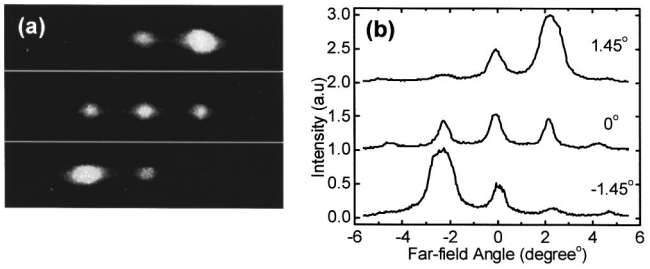

FIG. 3. (a) CCD image, and (b) far-field intensity pattern of a 6.9 $\times 13.6\ \mu m^2$ QPM–SHG NPC pumped by a Nd:YAG at an incident angle of 1.45°, 0°, −1.45°, respectively, and at a crystal temperature of 10 °C.

resolved, indicating a loss of phase-matching condition.

For a quantitative analysis of the earlier observations, we consider a ray tracing method in geometrical optics to resolve the reciprocal lattice vector effects on the spatial distribution of the QPM–SHG process. This is equivalent to solving a problem of $\mathbf{G}_{mn}(T,\phi)$, where the phase-matching temperature T becomes an index of the reciprocal lattice vector $\mathbf{G}_{mn}$ and the azimuth rotation angle ϕ in the $x-y$ plane. Here the material dispersion in the refractive index $n(\omega,T)$ is taken from Ref. 24 and a QPM condition of $\mathbf{k}_{2\omega}-2\mathbf{k}_{\omega}-\mathbf{G}_{mn}=0$ is used to evaluate the structure effect. Shown in Fig. 4 are the derived dispersion curves revealing the dependence of phase-matching temperature on the azimuth rotation angle. A general trend inferred from Fig. 4(a) of the 6.6 $\times 13.6\ \mu m^2$ period sample is a monotonic increase of phase-matching temperature with rotation angle. This finding agrees with most of the experimental observations except for the $G_{10}(T,\phi)$ assisted QPM–SHG process which is less sensitive to the variation of incident angle. On the other hand, we also have an increase of phase-matching temperature with

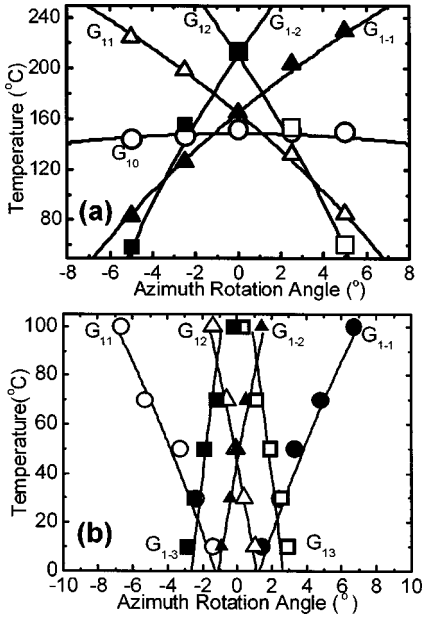

FIG. 4. Dispersion curves of $G_{mn}(T,\phi)$ illustrating the phase-matching temperature dependence on the azimuth rotation angle for the reciprocal lattice vector G_{mn} involved QPM–SHG process on NPC samples of (a) 6.6×13.6 and (b) 6.9×13.6 μm^2 period.

the magnitude of G_{mn} involved in the nonlinear wave interaction. This effect can further translate into an increase of far-field emission angle of the peak QPM–SHG signal in a direction *transverse* to the fundamental Nd:YAG pump beam. By increasing the lattice spacing in the structured $\chi^{(2)}$ nonlinearity, we note a linear dispersion relation on $\mathbf{G}_{mn}(T,\phi)$ can be maintained over the 6.9×13.6 μm^2 period sample of Fig. 4(b). The corresponding phase-matching temperature, however, is roughly lowered by a factor of 2 compared with that of the 6.6×13.6 μm^2 period sample of Fig. 4(a). Last but not least, we note the $\mathbf{G}_{m\pm n}(T,\phi)$ dispersion curves do reveal an axial symmetry as one varies the rotation angle in the $x-y$ plane. This can be related to the fact that the $\chi^{(2)}$ nonlinearity in the QPM–NPC has an orthorhombic lattice structure of C_{2v} symmetry.

In summary, we have demonstrated a promising route of constructing the $\chi^{(2)}$ QPM–NPCs by using the two-step poling technique. From the SHG measurement and geometric optics analysis, it is shown that the dispersion relation of $\mathbf{G}_{mn}(T,\phi)$ in the nonlinear wave generation process can be engineered by a suitable design of the lattice structure and periodicity of $\chi^{(2)}$ nonlinearity in the NPCs.

This research was supported by the National Science Council, Grant Nos. 91-2215-E-002-026 and 92-2215-E-002-013.

[1] M. Soljačić, M. Ibanescu, S. G. Johnson, Y. Fink, and J. D. Joannpoulos, Phys. Rev. E **66**, 055601(R) (2002).
[2] O. Painter, R. K. Lee, A. Scherer, A. Yariv, J. D. O'Brien, P. D. Dapkus, and I. Kim, Science **284**, 1819 (1999).
[3] C. B. Clausen, P. L. Christiansen, L. Torner, and Y. B. Gaidiei, Phys. Rev. E **60**, R5064 (1999).
[4] K. Sakoda and K. Ohtaka, Phys. Rev. B **54**, 5742 (1996).
[5] J. D. Joannopoulos, R. D. Meade, and J. N. Winn, *Photonic Crystals, Molding the Flow of Light* (Princeton University Press, Princeton, 1995).
[6] A. R. Cowan and J. F. Young, Phys. Rev. B **65**, 085106 (2002).
[7] A. Huttunen and P. Törmä, J. Appl. Phys. **91**, 3988 (2002).
[8] V. Berger, Phys. Rev. Lett. **81**, 4136 (1998).
[9] N. G. R. Broderick, G. W. Ross, H. L. Offerhaus, D. J. Richardson, and D. C. Hanna, Phys. Rev. Lett. **84**, 4345 (2000).
[10] A. Chowdhury, C. Status, B. F. Boland, T. F. Kuech, and L. McCaughan, Opt. Lett. **26**, 1353 (2001).
[11] J. R. Kurz, A. M. Schober, D. S. Hum, A. J. Saltzman, and M. M. Fejer, IEEE J. Sel. Top. Quantum Electron. **8**, 660 (2002).
[12] S. M. Saltiel and Y. S. Kivshar, Opt. Lett. **27**, 921 (2002).
[13] S.-N. Zhu, Y.-Y. Zhu, and N.-B. Ming, Science **278**, 843 (1997).
[14] J. A. Armstrong, N. Bloembergen, J. Ducuing, and P. S. Pershan, Phys. Rev. **127**, 1918 (1963).
[15] J. F. Nye, *Physical Properties of Crystals* (Oxford University Press, New York, 1989).
[16] For a recent review, please see in *Ferroelectric and Dielectric Thin Films Handbook of Thin Film Materials* vol. 3, edited by H. S. Nalwa (Academic, New York, 2002).
[17] R. C. Miller and G. Weinreich, Phys. Rev. **117**, 1460 (1960).
[18] R. G. Batchko, V. Y. Shur, M. M. Fejer, and R. L. Byer, Appl. Phys. Lett. **75**, 1673 (1999).
[19] K. Nassau, H. J. Levinstein, and G. M. Loiacono, J. Phys. Chem. Solids **27**, 989 (1966).
[20] L.-H. Peng, Y.-C. Fang, and Y.-C. Lin, Appl. Phys. Lett. **74**, 2070 (1999).
[21] K. Kitamura, Y. Furukawa, K. Niwa, V. Gopalan, and T. E. Mitchell, Appl. Phys. Lett. **73**, 3073 (1998).
[22] L.-H. Peng, Y.-J. Shih, and Y.-C. Zhang, Appl. Phys. Lett. **81**, 1666 (2002).
[23] L.-H. Peng, Y.-C. Shih, S.-M. Tsan, and C.-C. Hsu, Appl. Phys. Lett. **81**, 5210 (2002).
[24] D. H. Jundt, Opt. Lett. **22**, 1553 (1997).